PERGAMON

International Journal of Solids and Structures 37 (2000) 5745–5772

INTERNATIONAL JOURNAL OF SOLIDS and STRUCTURES

www.elsevier.com/locate/ijsolstr

Branching behavior in the nonlinear response of sandwich panels with a transversely flexible core

V. Sokolinsky, Y. Frostig*

Department of Civil Engineering, Technion, Israel Institute of Technology, 32000 Haifa, Israel

Received 23 March 1999; in revised form 11 August 1999

Abstract

A branching behavior of sandwich panels with a transversely flexible (''soft'') core subjected to longitudinal external forces is investigated using a geometrically nonlinear analysis. The study is based on a closed form high-order theory that allows for a general analysis without resort to the classical mode decoupling approach. The governing equations and the associated boundary conditions are presented, and the appropriate boundary conditions resulting from using edge beams are derived. An efficient path-following algorithm based on the quasi-Newton global framework has been developed. It provides a powerful numerical tool for determining the branching behavior which consists of a sequence of equilibrium states of the sandwich panel as a function of the external loading factor. Application of the general numerical analysis to the ''soft'' core sandwich panels reveals that they possess a complicated branching behavior with limit points and secondary bifurcations. It is shown that the wrinkling of the face sheets does not necessarily identify the buckling of the panel as a whole and in many cases it is a result of the nonlinear response. The localized buckling modes are found in some cases to be the critical ones rather than the usual sinusoidal buckling patterns. It is further shown that variations in the geometry, boundary conditions and mechanical properties of the panel constituents can lead to a qualitative shift in its nonlinear response from an imperfection-sensitive, ''shell-wise'' response, to an imperfection-nonsensitive, ''plate-wise'' one.

Keywords: Sandwich panels; Transversely flexible core; Geometrically nonlinear analysis; Edge beams; Localized buckling modes; Secondary bifurcations; Limit points

1. Introduction

The behavior of sandwich panels with a transversely flexible (''soft'') core is that of a *compound*

* Corresponding author: Fax: +972-4-323-433.
E-mail address: cvrfros@techunix.technion.ac.il (Y. Frostig).

0020-7683/00/$ - see front matter
PII: S0020-7683(99)00232-2

structure rather than an ordinary response of solid beams/panels. Such a structure combines three different layers into a single entity wherein the material properties of the core layer, especially its flexibility in the vertical direction, have a pronounced effect on its behavior. This flexibility leads to *local* and *localized* displacement patterns which can interact with an *overall* mode of the sandwich panel. The *local* response refers to a deformation pattern that is located at the face sheets only, such as wrinkling, whereas the *localized* response implies a deformation pattern which is confined to some zone along the face sheet. Thus, the buckling response of sandwich panels as a result of external longitudinal loads may be of the global, local or localized type, and their postbuckling response is much more complicated and complex than that of the ordinary panels. Nonlinear phenomena such as snap-through response, interactive mode buckling behavior as well as secondary bifurcations may occur and precautions must be taken when designing sandwich panels with a "soft" core.

The development of the theory of sandwich structures followed for long the classical approaches presented in detail in Allen (1969), Plantema (1966) and Zenkert (1995). Some authors have shown through experiments that there are considerable distinctions between the buckling response of sandwich panels with a honeycomb core and ordinary panels (see, for example, Harris and Nordby, 1969). The low mechanical properties of the core with respect to the facings suggested the use of elastic foundation techniques to analyze the local buckling response of the sandwich panel. At the same time, the global response was predicted by Euler's column formulas as a function of the facings mechanical properties only; occasionally, the contribution of the core shear rigidity was also included. Thus, the analysis and design of the sandwich panels is based on decoupling of the local and global responses while ignoring the *interaction* between them. As a result the critical design loads are based on the minimum between the overall and the local (wrinkling) buckling loads.

The local buckling response has been investigated by many researchers using various types of elastic foundation along with presumed sinusoidal modes (see Zenkert, 1995). Goodier and Hsu (1954) dealt with buckling of an *infinitely* long sandwich plate and showed that the nonsinusoidal modes, in which the deformation is confined to end zones of the plate, may occur with critical loads that are about one-half of those predicted on the basis of the sinusoidal mode. Moreover, the classical approaches use *nonrealistic* boundary conditions which are *incompatible* with the governing differential equations (i.e. the number of boundary conditions does not match an order of the differential equations) as indicated by Benson and Mayers (1967). They had justified that the classical treatment of the boundary conditions led to an incorrect performance assessment of the sandwich structures relative to the ordinary ones in practical applications. Another serious drawback of the classical approach consists in neglecting the influence of the transverse normal stresses that can be justified for the metallic incompressible cores, but is incorrect for the "soft" cores. As the modulus of elasticity of the core layer reduces with respect to the faces, the section of the sandwich becomes more flexible in the transverse direction giving rise to nonequal vertical deflections of the face sheets as well as to the appreciable peeling (transverse normal) and shear stresses in the core itself and at the face–core interface layers (see Frostig et al., 1992). In such circumstances the local and overall response modes essentially *interact* (see Hunt et al., 1988). Therefore, the decoupling of modes approach will lead to an absolutely *inadequate* simulation of the real behavior of sandwich panels. The effects of the peeling stresses have been incorporated into the sandwich analysis by very few authors (Benson and Mayers, 1967; Pearce and Webber, 1972) who, however, resorted to decoupling of the buckling response into symmetric and antisymmetric patterns and used the harmonic hypotheses ignoring thereby the *interaction* between the buckling modes. Furthermore, these formulations as before was incapable of adequate treatment of the *real* boundary conditions which are imposed on the upper and the lower faces at the *same* section of the panel. Hunt et al. (1988) had found the interactive response of the sandwich strut to be strongly unstable by the use of a simple mechanism that replaced the core with Winkler-type springs.

Frostig et al. (1992) and Frostig and Baruch (1993) proposed a refined closed form high-order

sandwich panel theory (HSAPT) which allows for analyzing a general sandwich lay-out with a "soft" core and is subjected to various types of external loading and boundary conditions including different conditions at the face sheets at the *same* section. The theory enables a *general* solution to be determined, i.e. the analysis does not separate the complicated sandwich response into isolated problems corresponding to the global and local modes. As a result the interactive mode response of an arbitrary complexity is automatically considered. The first reference deals with the general bending of a sandwich panel (Frostig et al., 1992) whereas the second one (Frostig and Baruch, 1993) is limited only to buckling of such structures and uses the linearized form of the geometrically nonlinear formulation derived to study the linear buckling response of the simply-supported sandwich panel with a membrane prebuckling stage. A photoelastic investigation conducted by Thomsen and Frostig (1997) demonstrated the close agreement between the experimental stress field, induced by the application of highly concentrated external loads or point supports with that determined by the HSAPT. Sokolinsky and Frostig (1997, 1998) have applied the HSAPT to study the *interactive* buckling and nonlinear response of the sandwich panels with a "soft" core and arbitrary supports subjected to nonmembrane regime in the prebuckling stage.

The present work uses the HSAPT to study the geometrically nonlinear *general* behavior of longitudinally compressed sandwich panels. The assumptions used are as follows: the panel constituents behavior is that of linear elastic materials; the face sheets, modeled by the ordinary panels (neglecting shear strains), are subjected to the intermediate class of deformations, i.e. large deformations, moderate rotations and small strains (see Novozhilov, 1953; Brush and Almroth, 1975); the core layer is assumed to be an *antiplane* medium with small deformations. Moreover, the height of a "soft" core is allowed to change under loading whereas its section plane does not remain plane. Since the modulus of elasticity and the flexural rigidity of the transversely flexible core are about three and two orders smaller than those of the faces, its longitudinal rigidity is neglected (see Frostig et al., 1992). The interface layers are assumed to resist shear and peeling stresses and provide full bonding between the core and face layers.

The nonlinear governing equilibrium equations and the associated boundary conditions are presented in the next chapter, along with the derivation of the appropriate boundary conditions for a panel supported by the edge beams. Next, the nonlinear numerical algorithm is described. Numerical examples of some typical simply-supported and cantilever panels with a "soft" core are analyzed and discussed, and conclusions are drawn.

2. Nonlinear equilibrium equations

The governing nonlinear differential equations for the sandwich panel with the "soft" core, and their associated boundary and continuity conditions as well as the core fields appear in Frostig and Baruch (1993) and are presented here for completeness.

The governing equations read:

$$N_{xxt,\,x} + b\tau = 0 \tag{1}$$

$$N_{xxb,\,x} - b\tau = 0 \tag{2}$$

$$M_{xxt,\,xx} + \left(N_{xxt} w_{t,\,x}\right)_{,x} + \frac{bE_c}{c}(w_b - w_t) + \frac{b(c + d_t)}{2}\tau_{,x} = -q_t \tag{3}$$

$$M_{xxb,\,xx} + \left(N_{xxb} w_{b,\,x}\right)_{,x} - \frac{bE_c}{c}(w_b - w_t) + \frac{b(c+d_b)}{2}\tau_{,x} = -q_b \tag{4}$$

$$u_{ot} - u_{ob} - \frac{c+d_t}{2} w_{t,\,x} - \frac{c+d_b}{2} w_{b,\,x} - \frac{c^3}{12E_c}\tau_{,xx} + \frac{c}{G_c}\tau = 0 \tag{5}$$

where the unknowns, u_{ot}, u_{ob}, w_t, w_b and τ, are the horizontal and the vertical displacements of the centroid line of the upper and the lower faces, and the shear stress in the core, respectively (see Fig. 1); $(\,)_{,x}$ denotes the derivative with respect to x, whereby x is implied any of three axes, x_t, x_b or $x_c (x_t = x_b = x_c = x)$; b, c, d_t, and d_b are geometrical characteristics of a panel section denoting the width of the section, the height of the core, and the thicknesses of the upper and the lower face, respectively (see Fig. 1(a)); G_c, E_c are the shear and the elastic moduli of the core; q_t, q_b are external distributed vertical forces applied to the upper and the lower face, respectively; N_{xxt}, N_{xxb}, M_{xxt}, and M_{xxb} are internal resultants, namely, the in-plane longitudinal forces and the bending moments in the upper and the lower face, respectively (see Fig. 1(b)).

The boundary conditions for the upper and the lower facings at the left ($x = 0$) and the right ($x = L$) edges are given below.

At the faces sheets ($i = t, b$):

$$\alpha N_{xxi} = N_i \quad \text{or} \quad u_{oi} = \bar{u}_{oi} \tag{6}$$

$$-\alpha M_{xxi} = M_i \quad \text{or} \quad w_{i,\,x} = \bar{w}_{i,\,x} \tag{7}$$

$$\alpha\left(M_{xxi,\,x} + N_{xxi} w_{i,\,x} + \frac{bd_i}{2}\tau\right) = P_i \quad \text{or} \quad w_i = \bar{w}_i \tag{8}$$

At the core:

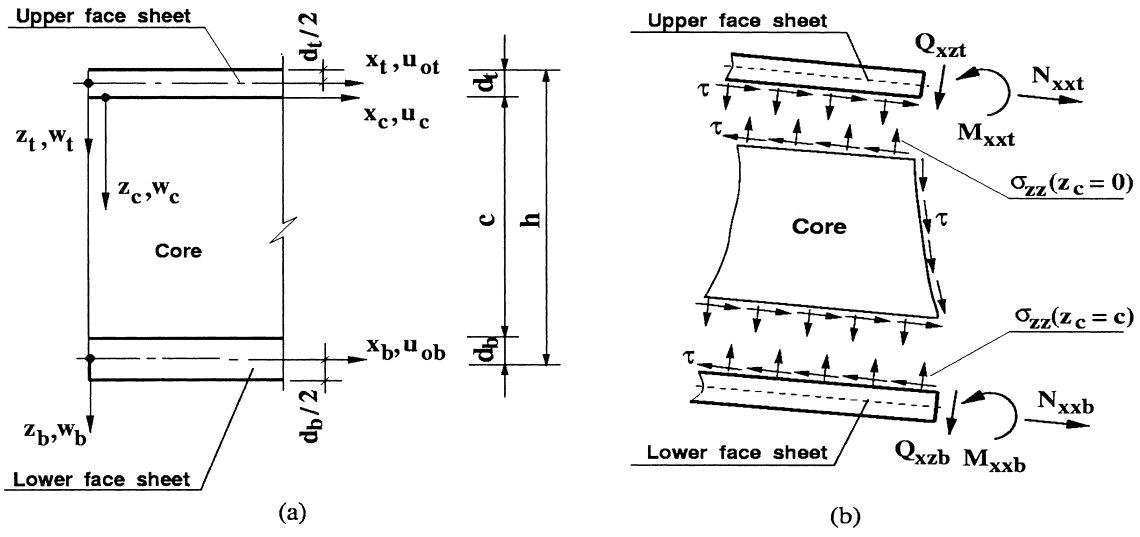

Fig. 1. Geometry (a) and internal resultants (b) of a sandwich panel.

$$\tau = 0 \quad \text{or} \quad w_c(x, z_c) = \bar{w}_c(z_c) \tag{9}$$

where L is the length of the panel; $\alpha = -1$ for $x = 0$ and $\alpha = 1$ for $x = L$; N_i, P_i and M_i are the horizontal and vertical external loads, and the external moments, respectively, applied at the faces; w_c is the unknown function of two variables, x and z_c, denoting the vertical displacement of an arbitrary point of the core; $\overline{u}_{oi}$, $\overline{w}_i$, and $\overline{w}_i, x$ are the specified values of the longitudinal and vertical displacements, and the angles of rotation at the faces boundaries, respectively; $\overline{w}_c$ are the specified vertical displacements through the thickness of the core edges.

The core fields in terms of the vertical stresses, and horizontal and vertical displacements, respectively, read:

$$\sigma_{zz}(x_c, z_c) = \frac{E_c}{c}(w_b - w_t) + \left(\frac{c}{2} - z_c\right)\tau_{,x} \tag{10}$$

$$u_c(x_c, z_c) = u_{ot} + \left(\frac{z_c^2}{2c} - z_c - \frac{d_t}{2}\right)w_{t,\,x} - \frac{z_c^2}{2c}w_{b,\,x} - \frac{z_c^2(3c - 2z_c)}{12E_c}\tau_{,xx} + \frac{z_c}{G_c}\tau \tag{11}$$

$$w_c(x_c, z_c) = \left(1 - \frac{z_c}{c}\right)w_t + \frac{z_c}{c}w_b - \frac{z_c(z_c - c)}{2E_c}\tau_{,x} \tag{12}$$

It should be emphasized that these stresses and deformation fields are the *result* of a closed form solution of the partial differential equations of equilibrium for the core. The term *panel* here applies either to a narrow beam or a wide beam (a plate in cylindrical bending). In case the face sheets are made of an isotropic material, the cylindrical bending of wide beams is accounted for by multiplying the Young's modulus of each face sheet by $1/(1 - \nu^2)$, where ν is the Poisson's ratio of the face sheet (Allen, 1969).

The boundary conditions for the special case where the sandwich panels are supported by edge beams are presented. An edge beam is a *rigid* diaphragm at the ends of the sandwich panel, where the support point A connecting the panel to the supporting devices may be located somewhere between the height of the panel rather than at the ends of the faces, see Fig. 2(a). Such supporting systems are widely used in practical applications to simplify the connection between the faces and the core of the sandwich panels with the supporting member of the panel.

The presence of an edge beam at the end of the sandwich panel yields:

$$w_t = w_b \tag{13}$$

$$w_{t,\,x} = w_{b,\,x} \tag{14}$$

$$w_{t,\,x} = \frac{u_{ot} - u_{ob}}{z_t + z_b} \tag{15}$$

$$w_t = w_c(x = 0, z_c) \tag{16}$$

where $z_t + z_b = c + d_t/2 + d_b/2$, see Fig. 2(a). Note that the above relationships exist regardless of the support type at the point A. The displacements and rotations at point A, see Figs. 2(c) and (d), can be expressed using the displacements and rotations of the faces as follows:

$$w_A = w_t \tag{17}$$

$$w_{A,\,x} = w_{t,\,x} \tag{18}$$

$$u_A = \frac{u_{ot} z_b + u_{ob} z_t}{z_t + z_b} \tag{19}$$

where u_A, w_A and $w_{A,\,x}$ are the displacements in the horizontal and vertical directions and the rotation, respectively, at the supporting point A. In order to derive the proper relations between local boundary conditions at the faces and the global ones at the point A, the expression for the internal potential energy is retained as given in Frostig and Baruch (1993), while the first variation of the external

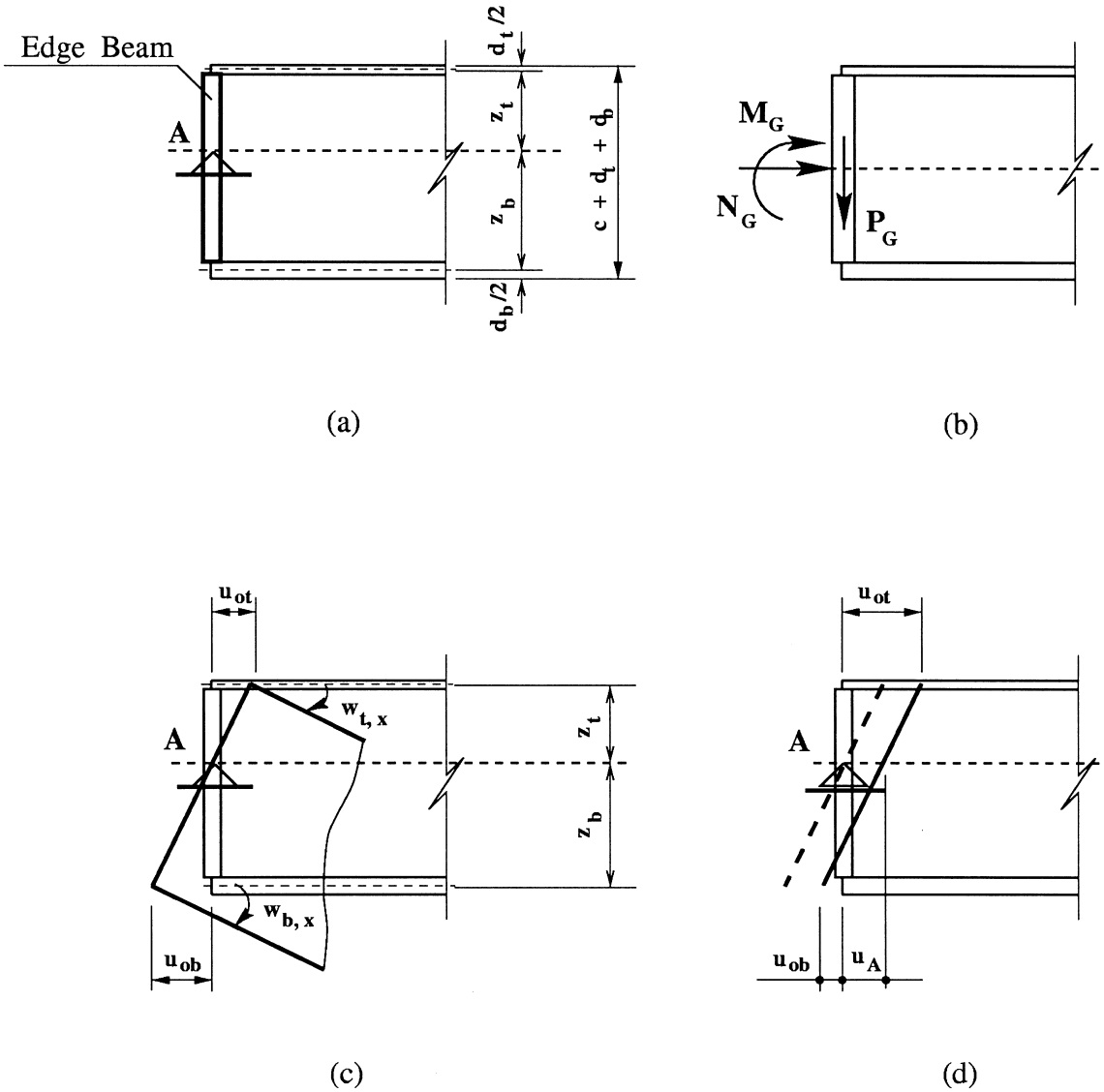

Fig. 2. Edge beam support: (a) Geometry; (b) Reactions at point A; (c) Displacement pattern of a hinge support; (d) Displacement pattern of a roller support.

potential energy presented there must be supplemented with

$$\delta V_{BC} = -\left(N_G \delta u_A + M_G \delta w_{A,\,x} + P_G \delta w_A\right) \tag{20}$$

here V_{BC} is the *part* of the external potential energy related to the left end supported by the edge beam; N_G, P_G and M_G are the global external concentrated forces in the horizontal and vertical directions, and the concentrated moment at the point A, see Fig. 2(b). Thus the appropriate boundary terms from the expression for the first variation of the total potential read:

$$\begin{aligned}\delta(U+V)_{BC} = & -N_{xxt}\delta u_{ot} - N_{xxb}\delta u_{ob} + M_{xxt}\delta w_{t,\,x} + M_{xxb}\delta w_{b,\,x} - \left(M_{xxt,\,x} + N_{xxt} w_{t,\,x}\right. \\ & \left. + \frac{bd_t}{2}\tau\right)\delta w_t - \left(M_{xxb,\,x} + N_{xxb} w_{b,\,x} + \frac{bd_t}{2}\tau\right)\delta w_b - \int_0^c b\tau\delta w_c \,\mathrm{d}z - \left(N_G \delta u_A \right. \\ & \left. + M_G \delta w_{A,\,x} + P_G \delta w_A\right) \\ = & \; 0\end{aligned} \tag{21}$$

for the case when the edge beam is attached to the left end of the panel. A similar expression can be determined also for the right edge. Substituting Eqs. (17)–(19) into the last equation yields:

$$\alpha[N_{xxt} + N_{xxb}] = N_G \quad \text{or} \quad u_A = u_G \tag{22}$$

$$\alpha[z_t N_{xxt} - z_b N_{xxb} - M_{xxt} - M_{xxb}] = M_G \quad \text{or} \quad w_{A,\,x} = w_{G,\,x} \tag{23}$$

$$\alpha\left[M_{xxt,\,x} + N_{xxt} w_{t,\,x} + M_{xxb,\,x} + N_{xxb} w_{b,\,x} + b(z_t + z_b)\tau\right] = P_G \quad \text{or} \quad w_A = w_G \tag{24}$$

$$\tau_{,x} = 0 \tag{25}$$

where u_G, w_G, and $w_{G,\,x}$ are the specified values of the deformations at the supporting point A. Thus, Eqs. (13)–(15) along with Eqs. (22)–(25) constitute the boundary conditions for the sandwich panel supported by the edge beams, where Eqs. (13)–(15) and (22)–(24) are the face conditions (compare with Eqs. (6)–(8)), and Eq. (25) is the core condition (compare with Eq. (9)). Note particularly that Eq. (25) is a straight consequence of the requirement,

$$\delta\int_0^c w_c \,\mathrm{d}z = 0, \tag{26}$$

stemming from Eq. (21) ($\tau \neq 0$ in this case), Eq. (12) for the vertical displacements of the core as well as Eqs. (13) and (16).

3. Nonlinear numerical analysis

The nonlinear governing differential equations (1)–(5) and the corresponding boundary conditions, (6)–(9) can be written as

$$\boldsymbol{L}(\boldsymbol{v}) = \boldsymbol{F} \tag{27}$$

where $\boldsymbol{L}$ is the nonlinear differential operator; $\boldsymbol{v} = \{u_{ot},\ u_{ob},\ w_t,\ w_b,\ \tau\}^{\mathrm{T}}$ is the vector function of the unknowns; $\boldsymbol{F}$ is the vector function of the external loading; and the symbol T denotes vector transpose. The exact continuous formulation of Eq. (27) is approximated by finite differences and it reads:

$$\boldsymbol{G}(\boldsymbol{u},\lambda) = \boldsymbol{0} \tag{28}$$

where $\boldsymbol{G}$ is the nonlinear algebraic operator from $\mathbb{R}^n \times \mathbb{R}$ to $\mathbb{R}^n$ in a finite dimensional space of size n; $\boldsymbol{u}$ is the n-dimensional vector of the unknowns; and λ is a load-level parameter that multiplies a *fixed* external loading vector, $\boldsymbol{G}_\lambda$, to yield the vector of external loads $\boldsymbol{q}$ at the current loading step.

It is emphasized that the choice of the type of discretization has been inspired by the lack of a finite element for the sandwich panel with a "soft" core in the library of modern finite element packages, and the presence of the highly stressed zones near the concentrated loads and in the vicinity of the support points. The complicated response at these regions is smeared by the finite elements (see Frostig and Baruch, 1990).

The system of nonlinear algebraic equations in Eq. (28) defines the equilibrium state of the sandwich panel. The equilibrium state is the point in $(\boldsymbol{u}, \lambda)$ space while the equilibrium branch is a connected curve consisting of such points. Evaluation of the nonlinear equilibrium path for the sandwich panel with a "soft" core is the main goal of the present work. The basic principles for an automatic path-following procedure can be found, for example, in Crisfield (1991, 1997), Keller (1987) and Seydel (1988). Note that the mixed formulation of the problem along with the chosen approximation technique require more general continuation procedures than those given in Crisfield (1997).

Choosing the load factor λ as the parameter of the equilibrium branch leads to the natural parameter continuation procedure for computing the solution curves of Eq. (28). Starting from the unloaded state of the structure the continuation procedure advances from one equilibrium state to another using the predictor–corrector technique. The path-following procedure in the present work implements the Euler tangential predictor

$$\tilde{\boldsymbol{u}}(\lambda_1) = \boldsymbol{u}_0 + (\lambda_1 - \lambda_0)\frac{\mathrm{d}\boldsymbol{u}_0}{\mathrm{d}\lambda} \tag{29}$$

with

$$\frac{\mathrm{d}\boldsymbol{u}(\lambda_0)}{\mathrm{d}\lambda} = \frac{\mathrm{d}\boldsymbol{u}_0}{\mathrm{d}\lambda} = -(\boldsymbol{G}_{\boldsymbol{u}})^{-1}\boldsymbol{G}_{\lambda,} \tag{30}$$

where $\tilde{\boldsymbol{u}} = \tilde{\boldsymbol{u}}(\lambda_1)$ is the predictor value of the solution vector $\boldsymbol{u}_1$ at the loading step λ_1; $(\boldsymbol{u}_0, \lambda_0)$ is any point on the equilibrium path; $\boldsymbol{G}_{\boldsymbol{u}}(\boldsymbol{u}_0, \lambda_0)$ is the Jacobian matrix; and $\boldsymbol{G}_\lambda$ is the vector of the partial derivatives of $\boldsymbol{G}$ with respect to the load parameter λ that is numerically equal to the fixed vector function of external loading (see Eq. (28)). The corrector step is based on the quasi-Newton global framework with line searches (see Dennis and Schnabel, 1983). This procedure, however, fails to trace the curve in the vicinity of the limit (turning) points. To permit the solution of such circumstances the natural parameter continuation must be abandoned in favor of some other type of parameterization strategy. Here the scalar normalization proposed by Keller (1977, 1987) has been used:

$$N(\boldsymbol{u}, \lambda, \Delta s) \equiv \frac{\mathrm{d}\boldsymbol{u}_0^{\mathrm{T}}}{\mathrm{d}s}(\boldsymbol{u} - \boldsymbol{u}_0) + \frac{\mathrm{d}\lambda_0}{\mathrm{d}s}(\lambda - \lambda_0) - \Delta s = 0 \tag{31}$$

where $(\frac{\mathrm{d}\boldsymbol{u}_0^{\mathrm{T}}}{\mathrm{d}s},\ \frac{\mathrm{d}\lambda_0}{\mathrm{d}s})$ is the unit tangent to the equilibrium path at the point $(\boldsymbol{u}_0, \lambda_0)$; Δs is the arclength distance from the point $(\boldsymbol{u}_0, \lambda_0)$. Combining Eqs. (28) and (31) produces an extended system of $n+1$ scalar equations for the $n+1$ unknowns $(\boldsymbol{u}, \lambda)$:

$$\begin{pmatrix} \boldsymbol{G}(\boldsymbol{u}, \lambda) \\ N(\boldsymbol{u}, \lambda, \Delta s) \end{pmatrix} = 0 \tag{32}$$

Computing the solution curve with the aid of the last system is known as the pseudoarclength continuation procedure (Keller, 1987). Then the predictor appears as

$$\tilde{\boldsymbol{u}}(s) = \boldsymbol{u}_0 + \Delta s \frac{\mathrm{d}\boldsymbol{u}_0}{\mathrm{d}s}, \tag{33}$$

$$\tilde{\lambda}(s) = \lambda_0 + \Delta s \frac{\mathrm{d}\lambda_0}{\mathrm{d}s} \tag{34}$$

As in the case of the natural parameter continuation, the corrector step is accomplished with the aid of the global quasi-Newton framework mentioned before. It is noted that the Jacobian of the augmented system, Eq. (32), remains nonsingular along the regular path even though the value of $\boldsymbol{G}_{\boldsymbol{u}}$ may be singular (as is the case at the limit points).

The computation of the tangent $(\frac{\mathrm{d}\boldsymbol{u}_0^{\mathrm{T}}}{\mathrm{d}s}, \frac{\mathrm{d}\lambda_0}{\mathrm{d}s})$ is an important part of the analysis and it defines the proper direction of advance along the path. The tangent vectors must satisfy the following conditions (see Keller, 1987):

$$\boldsymbol{G}_{\boldsymbol{u}} \frac{\mathrm{d}\boldsymbol{u}_0}{\mathrm{d}s} + \boldsymbol{G}_{\lambda} \frac{\mathrm{d}\lambda_0}{\mathrm{d}s} = 0, \tag{35}$$

$$\left\| \frac{\mathrm{d}\boldsymbol{u}_0}{\mathrm{d}s} \right\|^2 + \left| \frac{\mathrm{d}\lambda_0}{\mathrm{d}s} \right|^2 = 1 \tag{36}$$

with

$$\frac{\mathrm{d}\boldsymbol{u}_0}{\mathrm{d}s} = a\boldsymbol{\varphi}_{\boldsymbol{0}} \quad \text{and} \quad \frac{\mathrm{d}\lambda_0}{\mathrm{d}s} = a \tag{37}$$

The unknowns $\boldsymbol{\varphi}_{\boldsymbol{0}}$ and a are found through substitution of Eq. (37) into Eqs. (35) and (36) and they read:

$$\boldsymbol{G}_{\boldsymbol{u}} \boldsymbol{\varphi}_{\boldsymbol{0}} = -\boldsymbol{G}_{\lambda} \quad \text{and} \quad a = \frac{\pm 1}{\sqrt{1 + \|\boldsymbol{\varphi}_{\boldsymbol{0}}\|^2}} \tag{38}$$

In order to preserve the orientation of the path the sign in Eq. (38) is chosen to satisfy the inequality

$$a\left(\frac{\mathrm{d}\boldsymbol{u}_{-1}^{\mathrm{T}}}{\mathrm{d}s} \varphi_0 + \frac{\mathrm{d}\lambda_{-1}}{\mathrm{d}s} \right) > 0 \tag{39}$$

here $(\frac{\mathrm{d}\boldsymbol{u}_{-1}^{\mathrm{T}}}{\mathrm{d}s}, \frac{\mathrm{d}\lambda_{-1}}{\mathrm{d}s})$ is the preceding tangent vector.

The success of the numerical computations depends highly on a step length control. An efficient step control should combine sufficiently fast advance along the curve with reliable location of branching points (bifurcation and limit points). The latter is extremely important in the case of the sandwich structures under consideration where the branching points are often closely spaced (see below). Therefore, the present analysis uses additional devices that control the step length besides the usual restrictions on its maximum and minimum values and dependence on number of iterations for convergence at the previous step. The automatic choice of the method (natural parameter continuation

or pseudoarclength continuation) used here depends on the number of iterations ν required for convergence at the previous step, and the ratio ρ between the values of the derivatives $d\lambda/ds$ at the current point and the starting point of the path. In addition, the arclength technique can be chosen from the beginning. The natural parameter continuation is applied when $|\rho| \geq 0.7$ and $\nu \leq 5$, otherwise the pseudoarclength continuation is used. To ensure the proper location of the branching points, the ratio $\bar{\rho}$ is introduced:

$$\bar{\rho} = \frac{\dfrac{d\lambda_{-1}}{ds} - \dfrac{d\lambda_0}{ds}}{\dfrac{d\lambda_{-1}}{ds}} \tag{40}$$

where -1 and 0 denote the previous and the current points, respectively. As long as the value of $\bar{\rho}$ satisfies the inequality

$$\bar{\rho}_b \leq |\bar{\rho}| \leq \bar{\rho}_t, \qquad [\bar{\rho}_b, \bar{\rho}_t] \subset \mathbb{R}, \tag{41}$$

the increment of the step length is given by

$$\Delta_0 = \gamma 2^{\frac{4-\nu}{3}} \Delta_{-1}, \qquad \gamma \in \mathbb{R}, \tag{42}$$

where Δ_{-1} and Δ_0 are the increments of the governing parameter (load factor or arclength) at the previous and the current point, respectively; γ is a constant. A reduction in the ratio $|\bar{\rho}|$ below the lower bound $\bar{\rho}_b$ leads to doubling of the arclength distance, Δs, or increasing of the load factor by $1.3\Delta_{-1}$. An increase in $|\bar{\rho}|$ beyond the upper bound $\bar{\rho}_t$, on the other hand, causes the solution $(\boldsymbol{u}_0, \lambda_0)$ being currently determined to be disregarded, and the reduced value of the increment Δ to appear as:

$$\Delta_0 = \frac{\bar{\gamma}}{|\bar{\rho}|} \Delta_{-1}, \quad \bar{\gamma} \in \mathbb{R} \tag{43}$$

Furthermore, if the minimum value of the arclength that is prescribed a priori interferes with the reduction of Δ_0 expressed by the previous equation, it is halved until either Eq. (41) is satisfied or the arclength distance Δs is reduced below some control limit after which the computations are abnormally terminated. The use of the *two* lower bounds on the arclength distance has been adopted in order to prevent the premature slipping of Δs into small values, which slows down the advance along the path, as well as setting nonjustifiably high lower bound. It is noted that the value of the constant γ used in the numerical computations is $\gamma = 0.65$; the values of the parameters $\bar{\rho}_b$, $\bar{\rho}_t$ and $\bar{\gamma}$ generally depend on the value of $d\lambda_0/ds$ and they read

$$\bar{\rho}_b = 0.007, \quad \bar{\rho}_t = 0.3, \quad \bar{\gamma} = 0.15 \quad \text{for } \frac{d\lambda_0}{ds} \geq 10^{-4}, \tag{44}$$

and

$$\bar{\rho}_b = 0.007, \quad \bar{\rho}_t = 0.9, \quad \bar{\gamma} = 0.45 \quad \text{for } \frac{d\lambda_0}{ds} < 10^{-4} \tag{45}$$

The change of the determinant sign during continuation along the equilibrium path is used as the branching test function (see Keller, 1987 and Seydel, 1988). After the branching point is straddled, its value is determined by the bisection procedure. The test for a limit point or bifurcation at each singularity reads (see Keller, 1977):

$$\boldsymbol{\psi}^{\mathrm{T}}\boldsymbol{G}_{\lambda}\begin{cases}\approx 0 & \text{for bifurcation}\\ \neq 0 & \text{for a limit point}\end{cases} \tag{46}$$

where $\boldsymbol{\psi}$ is the left null vector of the Jacobian, $\boldsymbol{G}_{\boldsymbol{u}}$, at the singular point, whereas $\boldsymbol{G}_{\lambda}$ is the fixed vector of the external loading.

Switching branches at bifurcation points is performed using the method proposed by (Keller (1977, 1987)) which reflects the idea that if one branch through the simple bifurcation point is already computed, the tangent $(\frac{\mathrm{d}\boldsymbol{u}}{\mathrm{d}s}, \frac{\mathrm{d}\lambda}{\mathrm{d}s})$ at the bifurcation point on this branch is *known*. The solution on the emanating branch is sought with the aid of the $(n+1)$-dimensional vector $\boldsymbol{\zeta}$ which is "orthogonal" to the known tangent and lies in the plane spanned by vectors $(\boldsymbol{\phi}, 0)$ and $(\boldsymbol{\phi}_0, 1)$, where $\boldsymbol{\phi}$ is the right null vector of the Jacobian at the singular point, $\boldsymbol{G}_{\boldsymbol{u}}^{0}$ and vector $\boldsymbol{\phi}_0$ is defined by the system:

$$\boldsymbol{G}_{\boldsymbol{u}}{}^{0}\boldsymbol{\phi}_0 = -\boldsymbol{G}_{\lambda}$$

$$\boldsymbol{\psi}^{\mathrm{T}}\boldsymbol{\phi}_0 = 0 \tag{47}$$

The predictor is obtained by summing the vector $(\boldsymbol{u}^*, \lambda^*)$, denoting the bifurcation point, with $\boldsymbol{\zeta}$. Then the quasi-Newton procedure is used to solve the system similar to that of Eq. (32) with the scalar normalization N substituted by

$$N(\boldsymbol{u}, \lambda) = \boldsymbol{\zeta}^{\mathrm{T}}\boldsymbol{d}, \quad \boldsymbol{d} \in \mathbb{R}^{n+1} \tag{48}$$

The solution on the bifurcating branch is obtained by adding the vector $\boldsymbol{d}$ to the predictor. Once the first point on the bifurcating branch has been evaluated, the whole branch is computed in the same way as described above. Reversing the direction of the constructed orthogonal vector the other part of the bifurcating branch is obtained.

The equilibrium states which are close to the bifurcating branches can also be determined using the imperfection analysis as described in Brush and Almroth (1975) (in the mathematical literature it is also known as "perturbed bifurcation" method; see Keller, 1987). Giving the structure a small initial imperfection, the equilibrium branch can be evaluated bypassing the bifurcation point. The smaller the initial imperfection, the closer the "perturbed" equilibrium path to the bifurcating branch.

The nonlinear procedure outlined above has been implemented in a computer code "FSAN" developed in the "MATLAB" software environment (MATLAB, 1996).

4. Numerical study and discussions

A numerical study has been conducted on some typical simply-supported and cantilever sandwich panel configurations. The simply-supported lay-out adopted is the one that appears in Frostig and Baruch (1993). It consists of two face sheets metallic or symmetric composite laminated and a "soft" core made of foam or a low strength honeycomb and serves as a *basic* configuration. The parameters of the basic configuration are varied in the subsequent cases. The results of the numerical analysis are presented in the form of the branching (response) diagrams at selected sections along the panel span, which are supplemented by the displacement patterns for a better insight into the nonlinear behavior. The influence of the initial imperfections on the nonlinear sandwich response is also examined in all examples. The branching points are assigned numbers and are marked by bullets. The bifurcating branches are denoted by the uppercase letter "B" followed by one-digit or two-digit numbers as follows: in the case with one bifurcating branch a one-digit number denoting one of the two parts of the *same* branch emanating from a bifurcation point is used. In the case where several bifurcating branches exist

a two-digit number is used, where the first digit stands for the number of the bifurcating branch and the second one defines the number of its part.

4.1. Simply-supported sandwich panels

A simply-supported sandwich panel in Fig. 3 where the vertical deformations at the edges of the core are prevented, i.e. the shear stresses at the core edges exist, is studied (see Frostig and Baruch, 1993). The branching diagrams of the panel appear in Fig. 4 for two locations, namely, at midspan and in the vicinity of the right edge. As the critical buckling load at point 1, $N^1_{cr} = 9.38714$ kN, is reached the panel buckles into the wrinkling (local) mode (see Figs. 5(a) and 6(a)), with approximately 36 half waves similar to the results determined *analytically* by Frostig and Baruch (1993). The bifurcation point 1 is unstable (see Crisfield, 1997) and the panel exhibits a *snap-through* response that transfer it to a stable equilibrium state at point 4 or 5 (see Fig. 4). The displacement configurations corresponding to points 4 and 5 are given in Figs. 5(b) and 6(b), respectively. Thus, the snap-through response leads to disturbance of the pure sinusoidal mode (wrinkling mode) in such a way that the amplitudes of the vertical displacements of the facings grow toward the supports. Further increase in the load level along the bifurcating branch B1 emanating from the point 1 is possible along the curve B11 until a stable bifurcation point is reached, at point 6, or along the curve B12 at point 7. Note that before the *secondary* bifurcations at points 6 or 7 occur ($N^6_{bp} = N^7_{bp} = 9.40286$ kN), the response of the panel is *local*, see the midspan response in Figs. 4(a), 5(b) and 6(b). The displacement modes along the bifurcating branches B2 and B3 emanating from the points 6 and 7 appear in Figs. 5(c, d) and 6(c, d). Here the *interactive mode* buckling response consists of the local wrinkling mode which is coupled with the global one. Further increase in loading along the bifurcating branches B2 and B3 leads to a gradual reduction of the panel stiffness (see Fig. 4). It is interesting to note that the second buckling load, $N = 9.3979$ kN, on the trivial equilibrium path is in close proximity to the critical buckling load, N^1_{cr}, at the point 1 given above (these values have been verified *independently* using the linearized buckling analysis; see Sokolinsky and Frostig, 1999). Thus, when the bifurcation loads are closely spaced a snapping response at the critical load levels may occur.

An imperfection analysis of the panel has been carried out using fictitious distributed vertical forces $q_t = 10^{-6}$ kN/mm and $q_b = -q_t$ see Eqs. (3) and (4), which follow the sinusoidal buckling pattern of point 1. The results of the imperfection analysis are in close agreement with those of the "perfect" structure (see Fig. 7). The limit point 1 occurs at $N^1_{lp} = 9.38546$ kN and since it is unstable the panel exhibits the snapping behavior which carries it to a stable point, 3. A further continuation along the stable interval 3 – 4 follows the same behavior observed before along the curve B12 of the bifurcating branch B1. The bifurcation point 4 occurs at $N^4_{bp} = 9.40276$ kN that is close to the previous results.

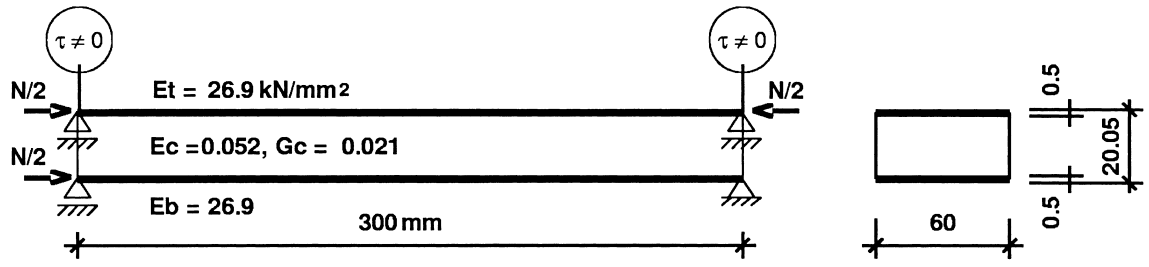

Fig. 3. Lay-out of simply-supported sandwich panel with non-free core edges (basic configuration)

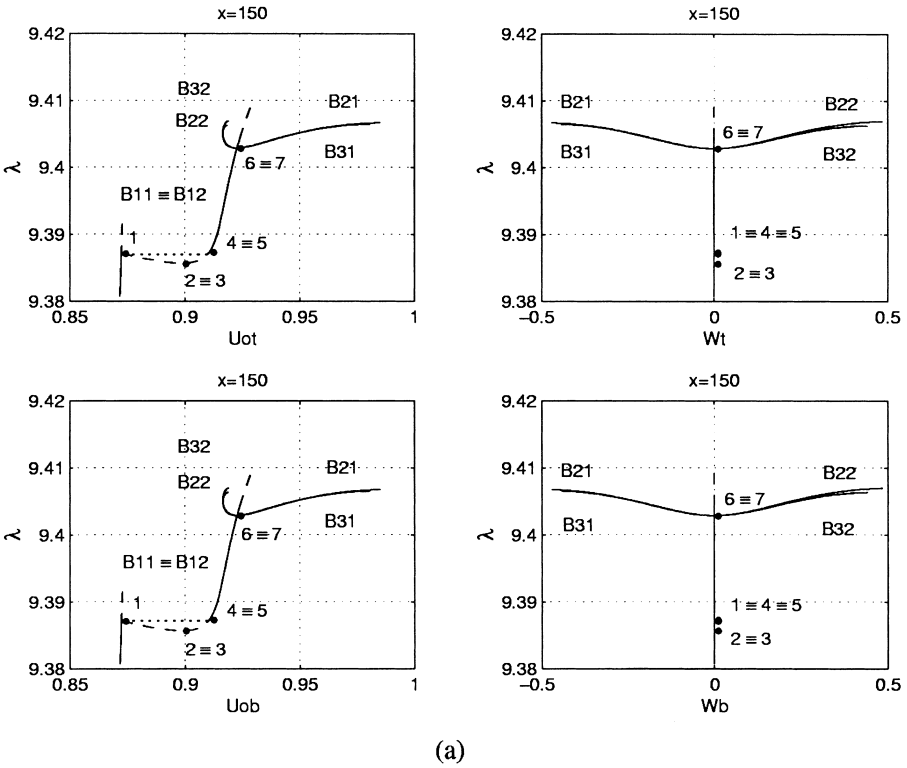

Fig. 4. Branching diagrams for simply-supported sandwich panel with non-free core edges: (a) at midspan; (b) in the vicinity of the right edge (— stable and - - unstable equilibrium states).

Note that small changes in the external loading may cause *appreciable* qualitative change in its behavior. This is illustrated by Figs. 4 and 7 where the difference in the magnitudes of the applied loads at the bifurcation point 1 and the limit points 2 and 3, see Fig. 4, is about 150 g (≈ 0.0015 kN), whereas it is about 40 g (≈ 0.0004 kN) only between the limit points 1 and 3 (see Fig. 7).

If the magnitudes of the fictitious loads q_t and q_b are increased by a factor of ten, the nonlinear response of the panel experiences some modifications although the basic features of the "perfect" behavior are still preserved (see Fig. 8). The continuation procedure along the main equilibrium path reveals three bifurcation points 1, 2 and 3 at load levels of 9.37388, 9.37496 and 9.40103 kN, respectively. Here, however, the first bifurcating branch leads to the second bifurcation point (point 2 in Fig. 8) along the path 1 – 4 – 5 – 2 on the one hand, and to the limit point 6 ($N^6_{\mathrm{lp}} = 9.3744$ kN) followed by a rapid reduction of the panel stiffness on the other hand. Therefore, it can be concluded that from the unstable bifurcation point 1 the panel snaps to point 5, then with an increase in the load

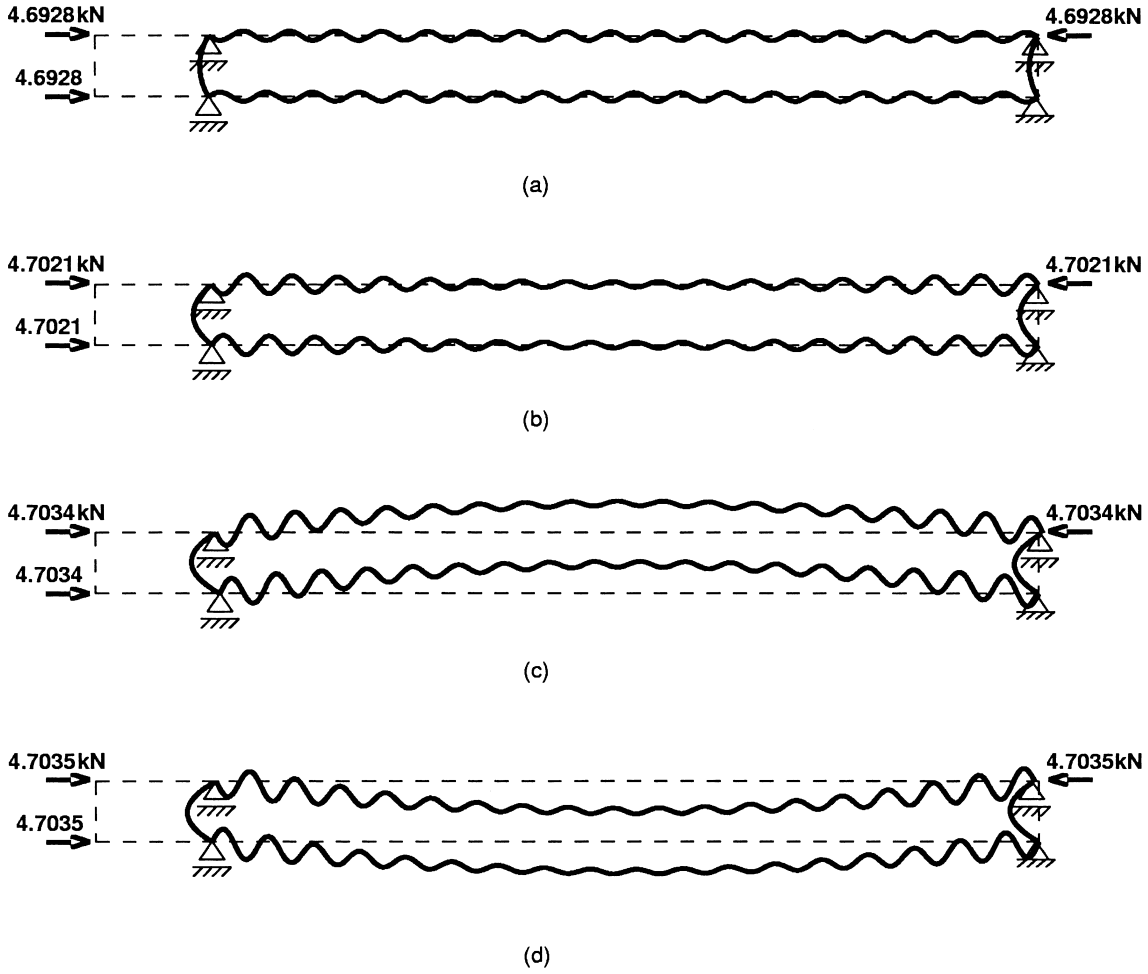

Fig. 5. Displacement patterns corresponding to the branching diagrams of Fig. 4: (a) at point 1 (to the right); (b) in range 4–6 of part B11 of the bifurcating branch B1; (c) on part B21 of the bifurcating branch B2; (d) on part B22 of the bifurcating branch B2.

factor λ it returns to the main equilibrium path at point 2 and further on to point 3 where the third bifurcating branch originates. Notice that the snapping response and the closely spaced bifurcation loads, points 1 and 2, are present together once again. However, here the snap-through behavior leads to an interactive mode response (see Fig. 9(a)), where the global buckling mode of one sine half wave interacts with the wrinkling pattern induced by the fictitious loading. The global mode diminishes gradually along interval 5 – 2, as expected, since the main equilibrium path is characterized by a local response only. The local response along the interval 2 – 3 closely resembles that of the "perfect" panel along interval 5 – 7 (see Fig. 4), where the amplitudes of the vertical displacements are larger toward the supports. The interactive mode response along the third bifurcating branch starting from point 3 is also similar to the behavior of the "perfect" panel along the bifurcating branch B2 Figs. 6(c) and (d). It can be concluded that the sandwich panel discussed is an *imperfection-sensitive* structure. This conclusion naturally follows from the results of the imperfection analysis on the one hand, and from the instability of the equilibrium state at the bifurcation point 1 (see Fig. 4), on the other hand.

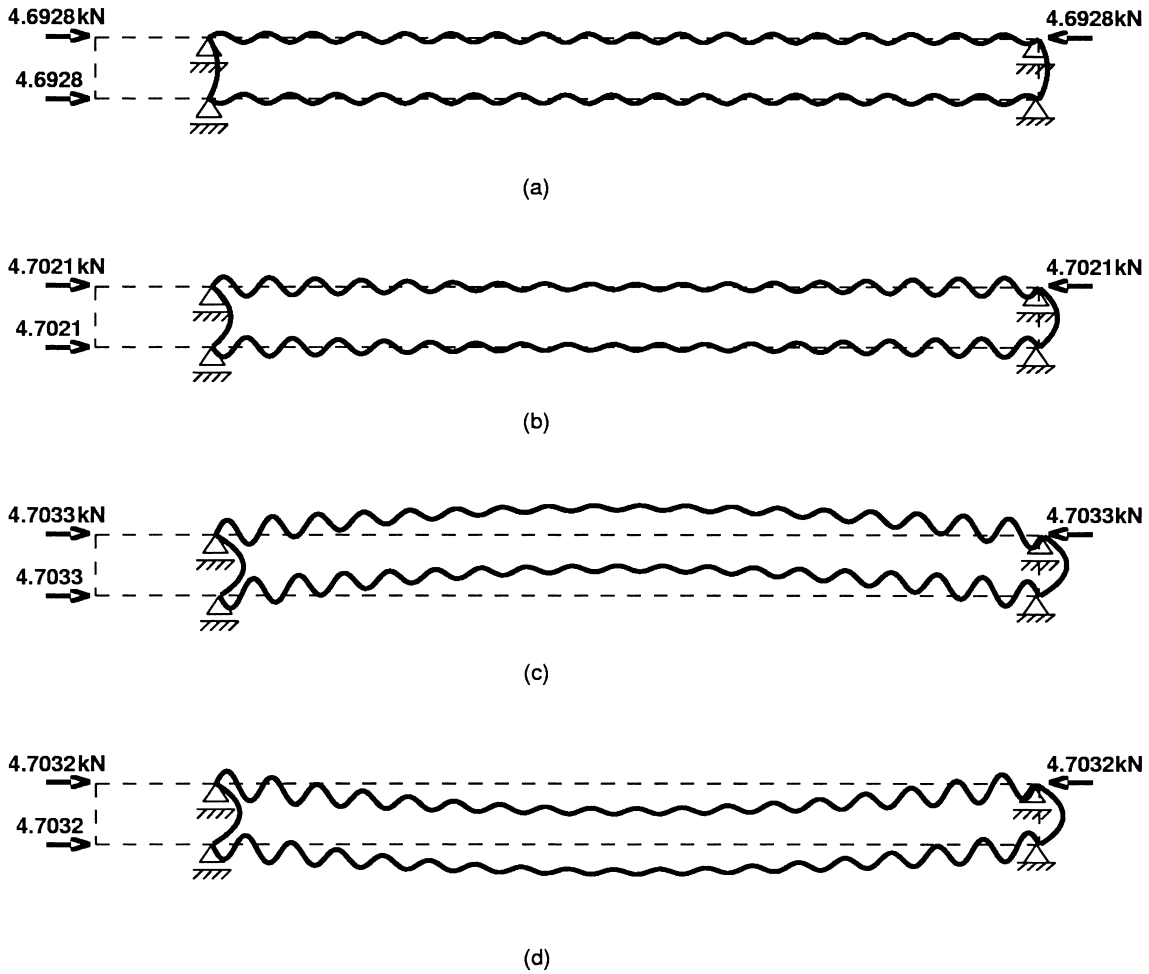

Fig. 6. Displacement patterns corresponding to the branching diagrams of Fig. 4: (a) at point 1 (to the left); (b) in range 5–7 of part B12 of the bifurcating branch B1; (c) on part B31 of the bifurcating branch B3; (d) on part B32 of the bifurcating branch B3.

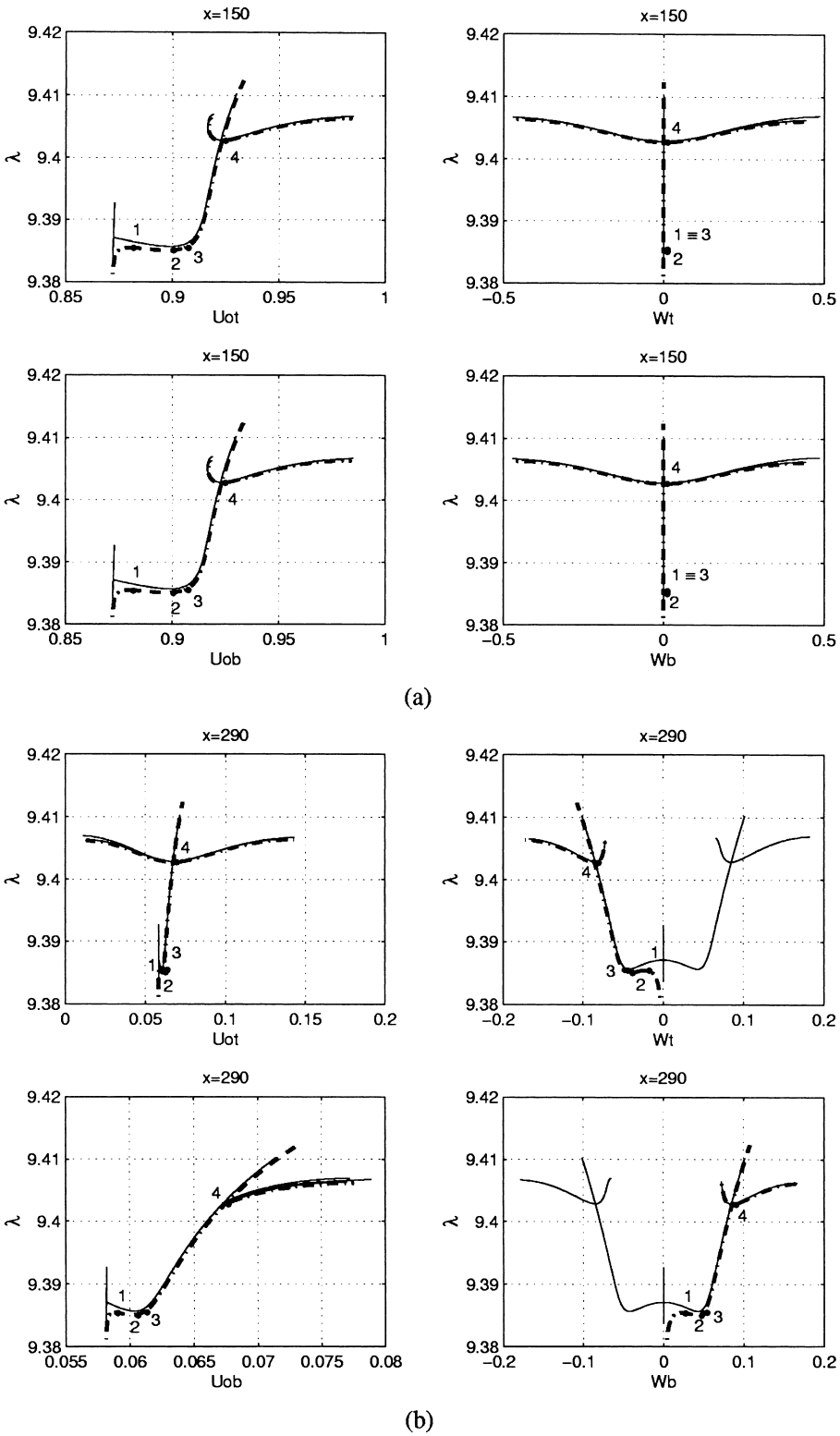

Fig. 7. Results of imperfection analysis vs. the "perfect" response for simply-supported sandwich panel with non-free core edges, $|q_t| \approx 10^{-6}$: (a) at midspan; (b) in the vicinity of the right edge (— "perfect" response; -. stable and - - unstable equilibrium states for imperfection analysis).

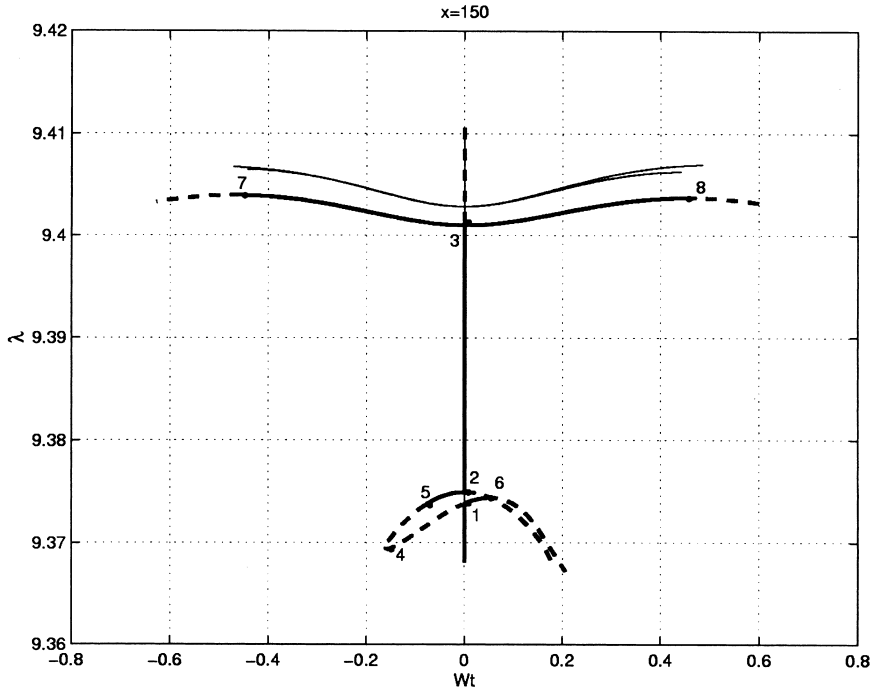

(a)

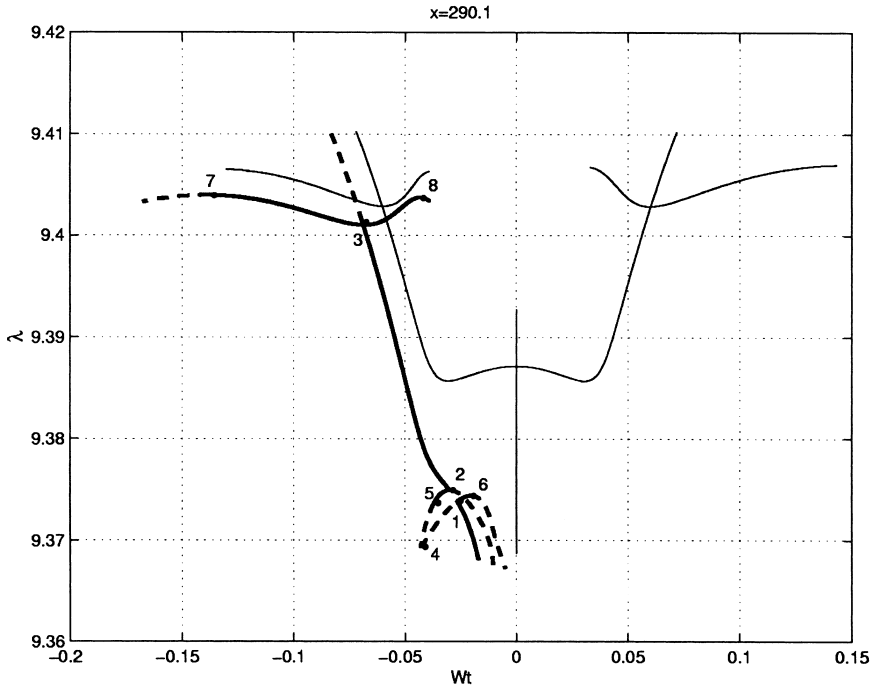

(b)

Fig. 8. Results of imperfection analysis (bold lines) vs. the "perfect" response (thin lines) for simply-supported sandwich panel,with non-free core edges, $|q_t \approx 10^{-5}$: (a) at midspan; (b) in the vicinity of the right edge (— stable and - - unstable equilibrium states)

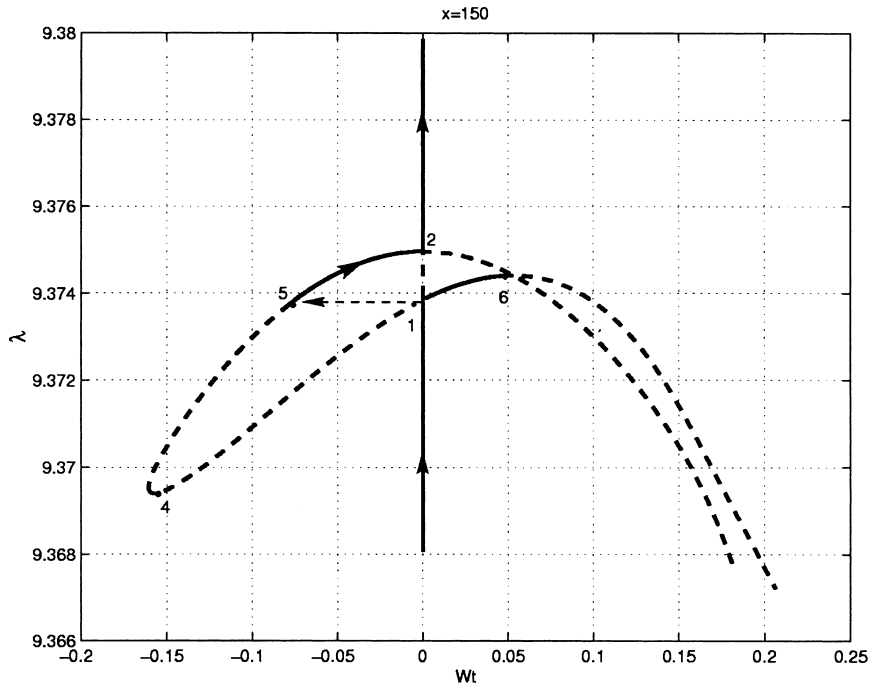

(a)

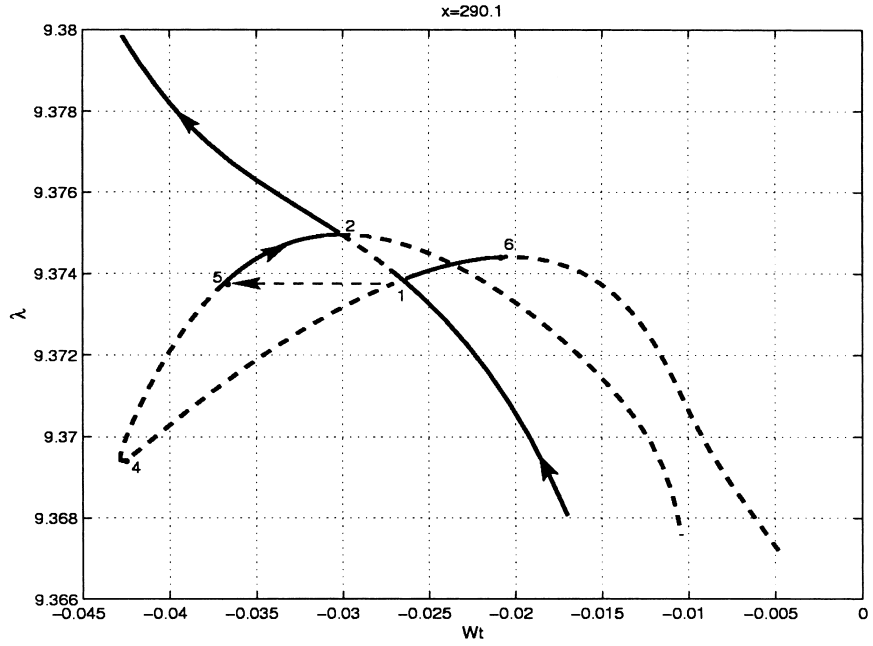

(b)

Fig. 9. Zooms in the vicinity of the bifurcation point 2 of Fig. 8: (a) at midspan; (b) in the vicinity of the right edge.

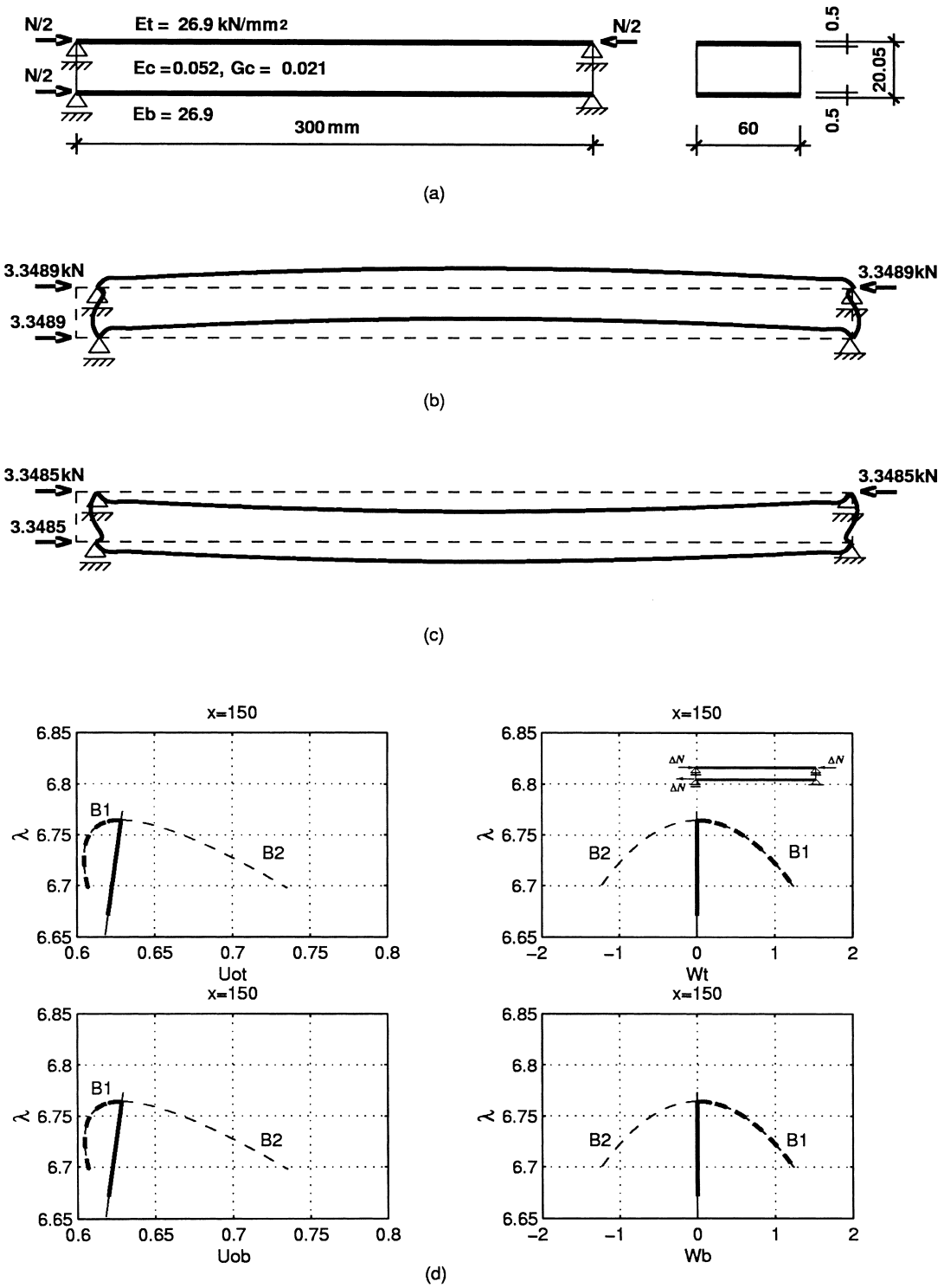

Fig. 10. Simply-supported sandwich panel with free core edges: (a) configuration; (b) displacement pattern on part B2 of the bifurcating branch; (c) displacement pattern on part B1 of the bifurcating branch; (d) branching diagrams at midspan for the "perfect" (thin lines) and imperfect (bold lines) structure (—— stable and - - unstable equilibrium states).

A strong qualitative change is achieved by merely removing the restrictions on the vertical displacements of the core at the ends of the panel (see Fig. 10(a)); thus the edges of the core are free of shear stresses. The resulting *subcritical pitchfork* bifurcation (see Seydel, 1988) appears in Fig. 10(d). Notice that the second bifurcation load ($N = 7.0738$ kN) is now quite different from the critical buckling load, $N_{cr} = 6.76439$ kN. The critical buckling behavior in this case consists of a *nonsinusoidal* buckling mode where the deformations are confined to the end zones of the panel and are also known as "*localized buckling mode*" (see Figs. 10(b) and (c)). The critical load level is much lower when compared with the sinusoidal one, namely $N_{sin}/N_{cr} = 1.3877$. The results of the imperfection analysis are shown in the branching diagrams of Fig. 10(d) with thick lines. They have been determined with the aid of the fictitious edge couples induced by small longitudinal forces, $\Delta N \approx 10^{-6}$ kN, applied at the facings.

The transversely flexible core has a pronounced effect on the behavior of sandwich structures (see Frostig et al., 1992; Frostig and Baruch, 1993; Sokolinsky and Frostig, 1999). The panel in Fig. 11(a) buckles into the global mode of Figs. 11(b) and (c) exhibiting the subcritical pitchfork behavior ($N_{cr} = 12.5472$ kN); see Fig. 11(d). Notice that the ratio E_c/G_c coincides with its counterpart for the basic lay-out. The critical *buckling* response here can be readily compared with that determined analytically and represented in a graphic form by Frostig and Baruch (1993). The important distinctive feature of the present nonlinear response is the sharp drop in the panel stiffness at some values of the load factor λ. The results of the imperfection analysis are determined with the aid of the fictitious uniform load q_t of the order of 10^{-6} kN/mm.

The nonlinear behavior of the sandwich panel with edge beams appears in Fig. 12. The edge beams prevent the formation of the wrinkling waves near the supports and cause the amplitudes of the vertical displacements of the facings to grow toward the flexible center (see Figs. 12(b) and (c)). The critical buckling load, $N_{cr} = 9.40102$ kN, is close to the *secondary* bifurcation points of the first example (points 6, 7 in Fig. 4), but here the bifurcation point is unstable (see Fig. 12(d)). In the next case the location of the supports through the thickness of the panel has been changed (see Fig. 13(a)) and the branching diagrams possess a limit point at $N_{lp} = 8.29054$ kN (see Figs. 13(d) and 14 with end shortening diagram). It is important to notice that since the sandwich panel is a *compound* structure, the wrinkling of the facings does not necessarily reflect buckling of the whole structure, (see Fig. 13(b) and (c)). Here an *interactive mode* nonlinear response consisting of overall and wrinkling modes exists.

4.2. Cantilever sandwich panels

The simply-supported boundary conditions of the basic lay-out are replaced by the clamped-free boundary conditions (see Fig. 15(a)). Here the external longitudinal forces are exerted on the face sheets only, and the boundary conditions at the loaded edge consist of the longitudinal forces of magnitude $N/2$, null bending moments and shear resultants in the upper and lower faces as well as null shear stresses in the core. Two cantilever panels that differ only in their heights have been investigated (see Figs. 15(a) and 16(a)). The critical buckling mode of the panel with the height of $h = 20.05$ mm is *global*, (Figs. 16(b) and (c)), while the critical buckling mode of the panel with the augmented height, $h = 23.05$ mm, is *localized*, (Fig. 15(b) and (c)). It is interesting to note, however, that the situation is opposite for the second buckling mode.

The cantilever panel with the augmented height, see Fig. 15(a), exhibits the subcritical pitchfork behavior, and is an *imperfection-sensitive* structure, see Fig. 15(d). The imperfection analysis has been carried out with the aid of two fictitious concentrated moments of the order of 10^{-5} kN mm applied to the facings at the loaded edge, see Eq. (7).

The cantilever panel with the height of the basic configuration (see Fig. 16(a)), yields a *supercritical pitchfork* response (see Fig. 16(d)). There is an exchange of stability from the trivial equilibrium path to the bifurcating branch at the bifurcation point. The imperfection analysis, accomplished with the aid of

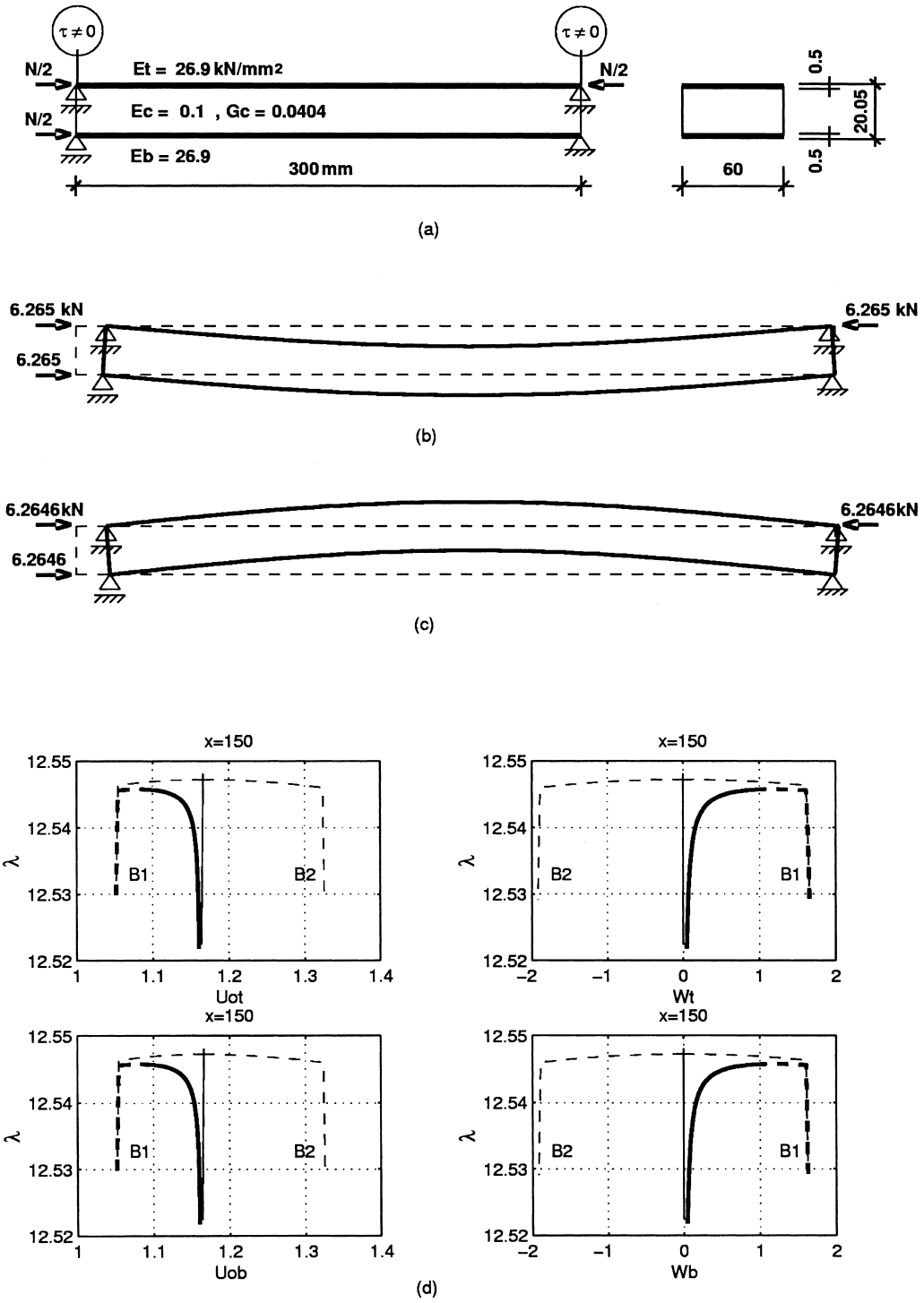

Fig. 11. Simply-supported sandwich panel with non-free core edges and a stiffer core: (a) configuration; (b) displacement pattern on part B1 of the bifurcating branch; (c) displacement pattern on part B2 of the bifurcating branch; (d) branching diagrams at mid-span for the "perfect" (thin lines) and imperfect (bold lines) structure (— stable and - - unstable equilibrium states).

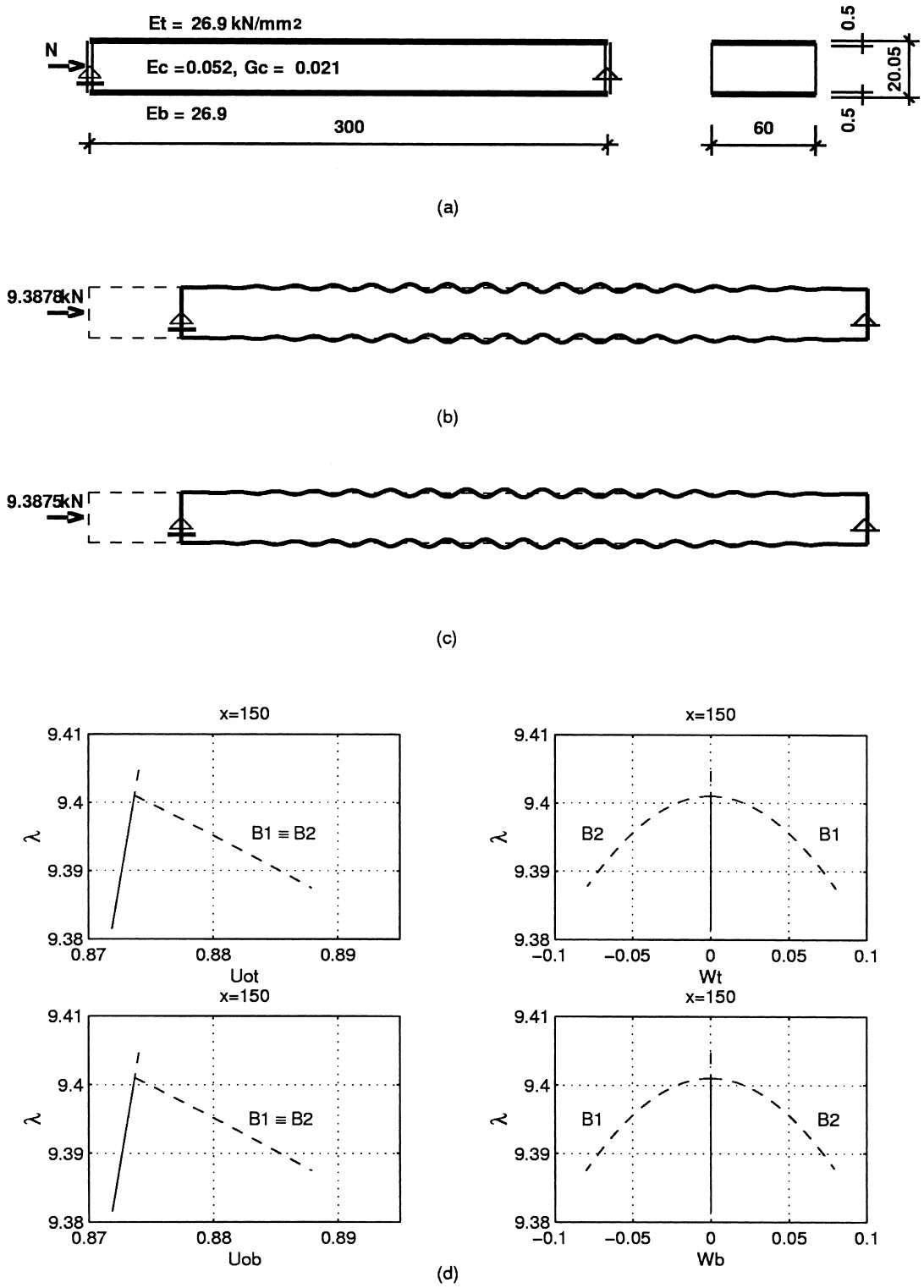

Fig. 12. Simply-supported sandwich panel with edge beams: (a) configuration; (b) displacement pattern on part B2 of the bifurcating branch; (c) displacement pattern on part B1 of the bifurcating branch; (c) branching diagrams at midspan (— stable and - - unstable equilibrium states).

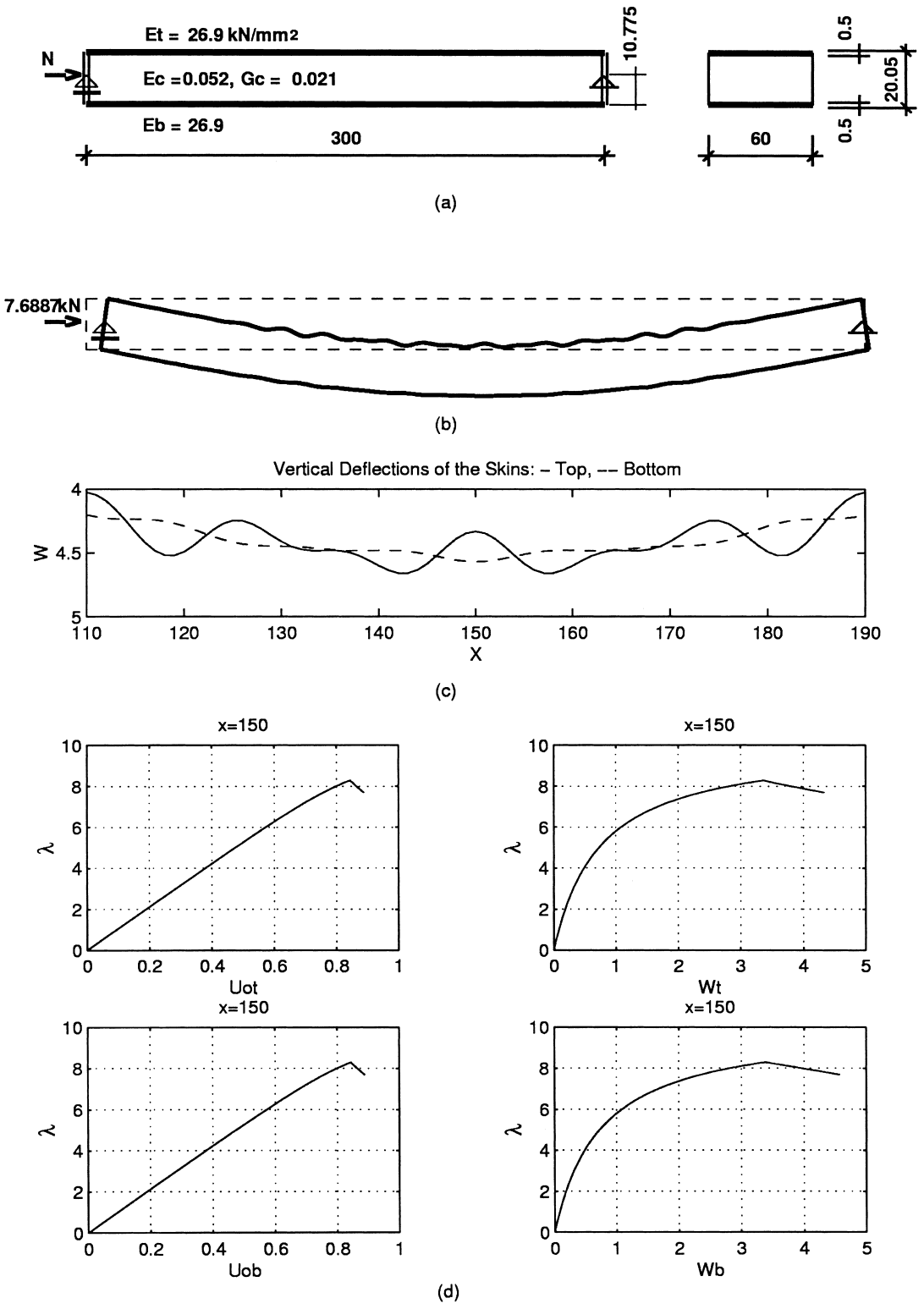

Fig. 13. Simply-supported sandwich panel with edge beams and eccentric supports (a) configuration; (b) displacement pattern; (c) interactive response at midspan; (d) branching diagrams at midspan

the fictitious uniform load $q_t \approx 10^{-6}$ kN/mm, reveals that the sandwich panel in this case is *not* imperfection sensitive. The same conclusion can be reached regarding the stable equilibrium state at the bifurcation point.

5. Conclusions

The geometrically nonlinear analysis of the longitudinally loaded sandwich panels with a transversely flexible core, based on the closed form high-order sandwich panel theory (HSAPT), is presented. The path-following procedure developed performs well and can be efficiently used to predict the nonlinear response of the sandwich panels with a transversely flexible core for practical applications.

The nonlinear analysis of the various panels reveals that the wrinkling of the facings does not *necessarily* means that the panel as a *whole* has buckled since the the sandwich panel is a *compound* structure. It actually deforms in such a way that the triggering overall mode gradually transforms into

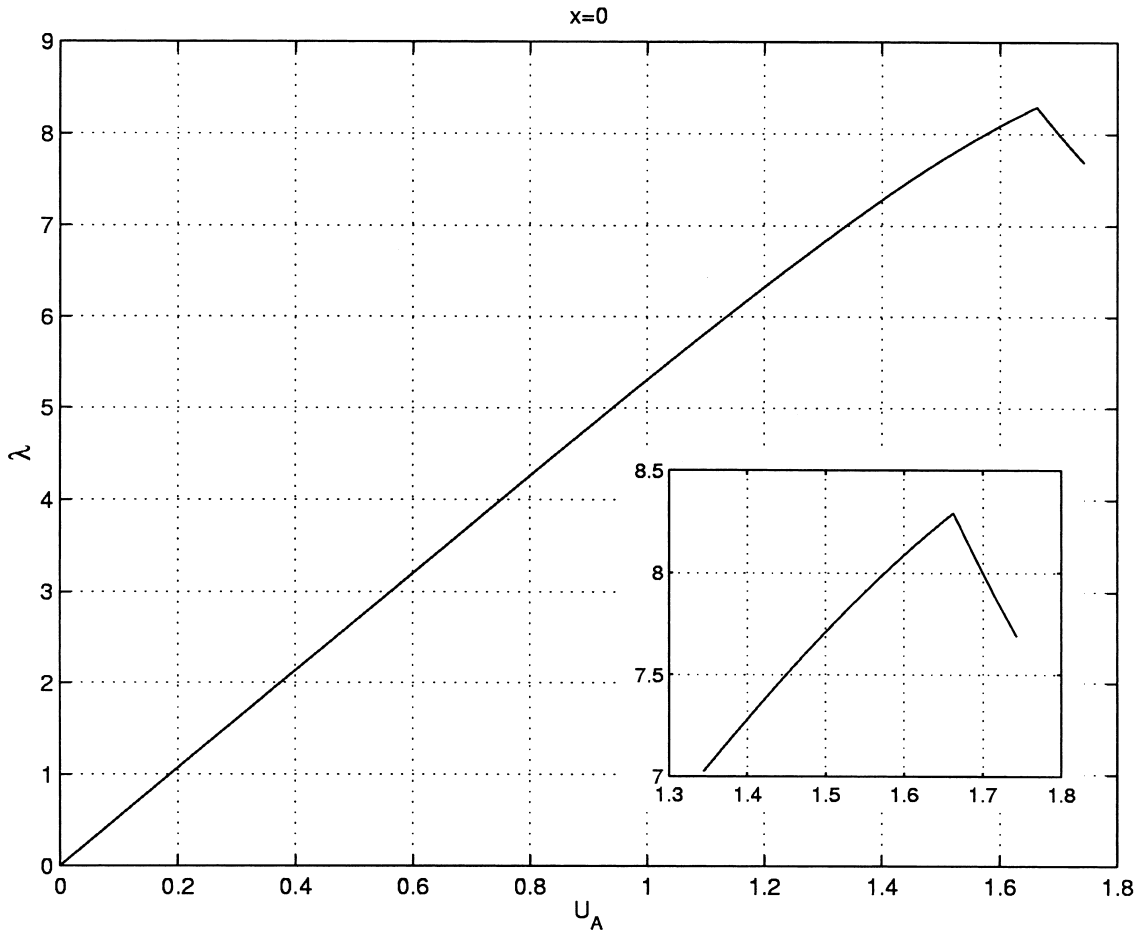

Fig. 14. End shortening in case of an edge beam (see Fig. 13).

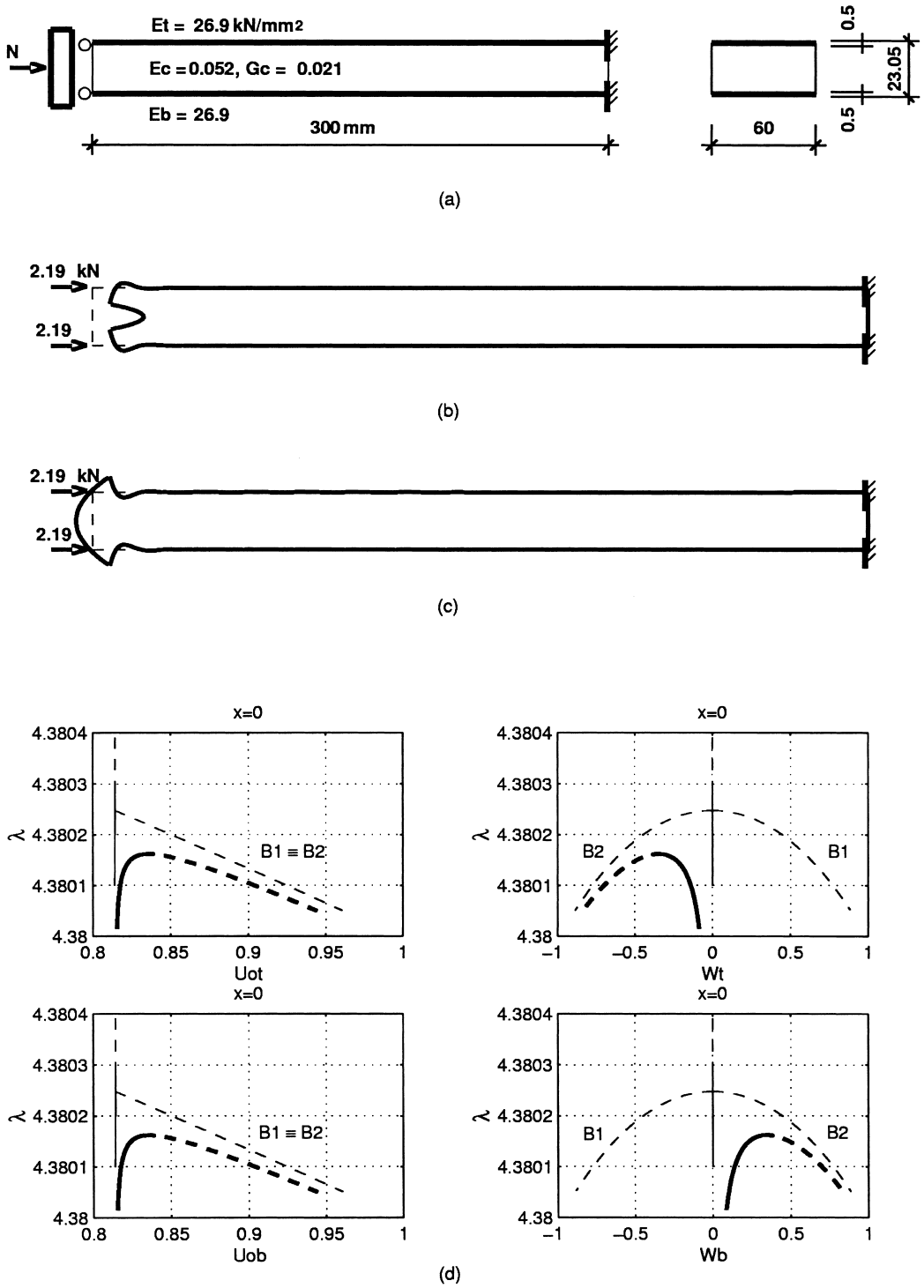

Fig. 15. Cantilever sandwich panel with augmented height: (a) configuration; (b) displacement pattern on part B1 of the bifurcating branch; (c) displacement pattern on part B2 of the bifurcating branch; (d) branching diagrams at the free end for the "perfect" (thin lines) and imperfect (bold lines) structure (— stable and - - unstable equilibrium states).

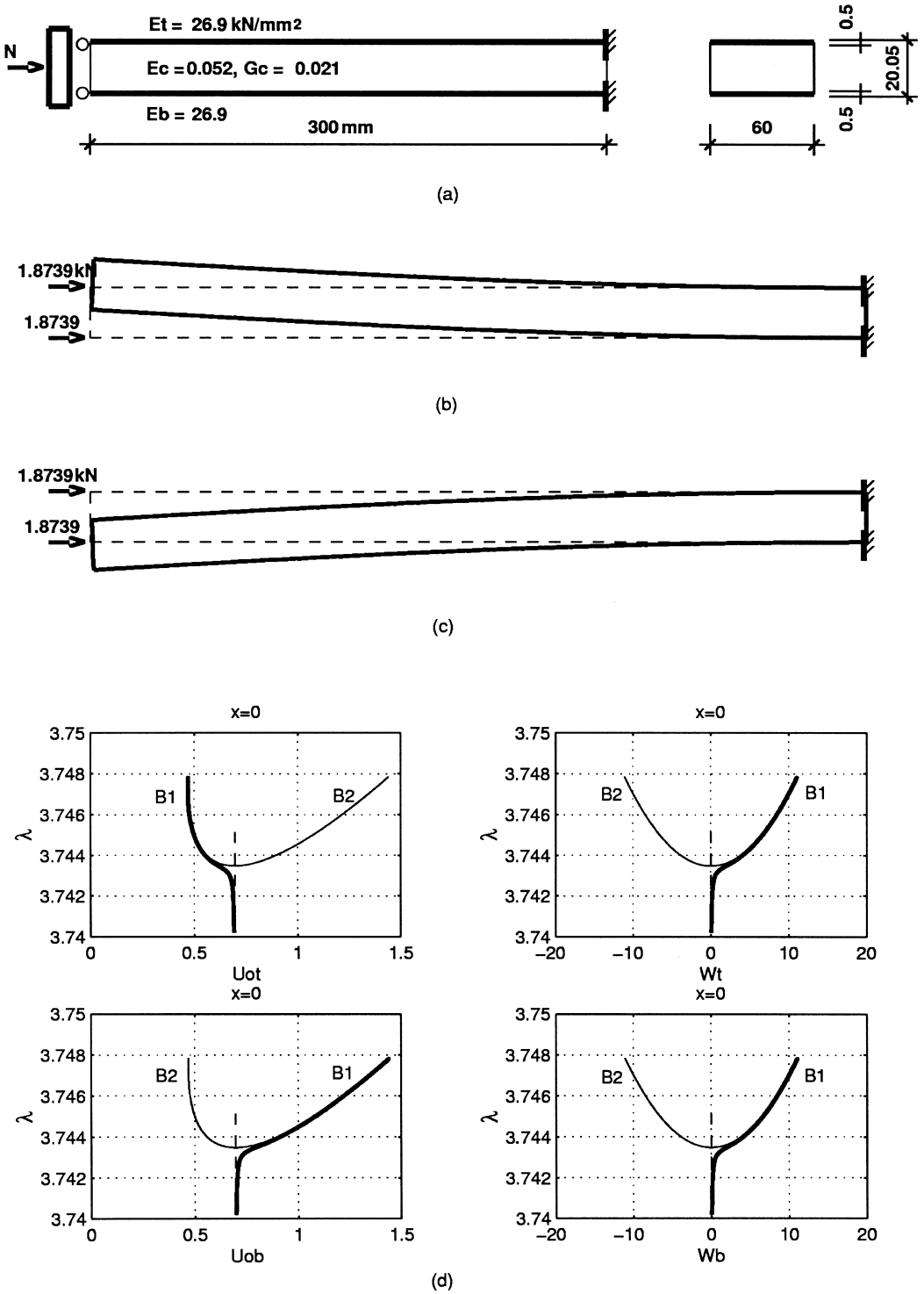

Fig. 16. Cantilever sandwich panel: (a) configuration; (b) displacement pattern on part B2 of the bifurcating branch; (c) displacement pattern on part B1 of the bifurcating branch; (d) branching diagrams at the free end for the "perfect" (thin lines) and imperfect (bold lines) structure (— stable and - - unstable equilibrium states).

the interactive mode displacement configuration along the *same* equilibrium path. The special features of this response are caused by the interaction of the face sheets with the transversely flexible core.

The stability analysis demonstrates that the *nonsinusoidal* modes confined to the support zones of the panel (localized modes) may occur at critical loads much lower than those predicted on a basis of *assumed* sinusoidal modes. Such localized behavior is not amenable to the approaches based on the decoupling of modes techniques.

The nonlinear study reveals that variations in the geometry of the sandwich panel and in its boundary conditions as well as in the mechanical properties of its constituents — individually and/or in combination — may lead to qualitative change in the panel behavior. Such a change manifests itself as shifting of the panel response from an imperfection-sensitive "shell-wise" response to an imperfection-nonsensitive "plate-wise" one. Consequently it is not known a priori, before the nonlinear analysis is conducted, which category of instability the structure belongs to — imperfection-sensitive or imperfection-nonsensitive. This feature does not exist in ordinary solid beams/panels used in engineering practice and may suggest the introduction of some knock-down factors in the design of sandwich panels with a transversely flexible core.

References

Allen, H.G., 1969. Analysis and Design of Structural Sandwich Panels. Pergamon Press, London.

Benson, A.S., Mayers, J., 1967. General instability and face wrinkling of sandwich plates — unified theory and approach. AIAA Journal 5 (4), 729–739.

Brush, Don O., Almroth, Bo O., 1975. Buckling of Bars, Plates and Shells. McGraw-Hill, New York.

Crisfield, M.A., 1991. Nonlinear Finite Element Analysis of Solids and Structures, Vol. 1: Essentials. Wiley, Chichester.

Crisfield, M.A., 1997. Nonlinear Finite Element Analysis of Solids and Structures, Vol. 2: Advanced Topics. Wiley, Chichester.

Dennis, J.E., Schnabel, R.B., 1993. Numerical Methods for Unconstrained Optimization and Nonlinear Equations. Prentice-Hall, Englewood Cliffs, NJ.

Frostig, Y., Baruch, M., 1990. Bending of sandwich beams with transversely flexible core. AIAA Journal 28 (3), 523–531.

Frostig, Y., Baruch, M., Vilnay, O., Sheinman, I., 1992. High-order theory for sandwich-beam behavior with transversely flexible core. Journal of the Engineering Mechanics Division, ASCE 118 (5), 1026–1043.

Frostig, Y., Baruch, M., 1993. High-order buckling analysis of sandwich beams with transversely flexible core. Journal of the Engineering Mechanics Division, ASCE 119 (3), 476–495.

Goodier, J.N., Hsu, C.S., 1954. Nonsinusoidal buckling modes of sandwich plates. AIAA Journal 21 (8), 525–532.

Harris, B.J., Nordby, G.M., 1969. Local Failure of Plastic-foam Core Sandwich Plates. Journal of the Structural Division, ASCE 95 (4), 585–610.

Hunt, G.W., da Silva, L.S., Manzocchi, G.M.E., 1988. Interactive buckling in sandwich structures. Proceedings of the Royal Society of London. A. Mathematical and Physical Sciences 417, 155–177.

Keller, H.B., 1977. Numerical solution of bifurcation and nonlinear eigenvalue problems. In: Rabinowitz, P.H. (Ed.), Applications of Bifurcation Theory. Academic Press, New York, pp. 359–384.

Keller, H.B., 1987. Numerical Methods in Bifurcation Problems. Tata Institute of Fundamental Research, Bombay.

MATLAB, 1996. MATLAB Reference Guide, Version 5. Math Works Inc, Natick, MA.

Novozhilov, V.V., 1953. Foundations of the Nonlinear Theory of Elasticity. Graylock Press, Rochester, NY.

Pearce, T.R.A., Webber, J.P.H., 1972. Buckling of Sandwich Panels with Laminated Face Plates. Aeronaut. Quart. 23 (5), 148–160.

Plantema, F.J., 1966. Sandwich Construction. Wiley, New York.

Seydel, R., 1988. From Equilibrium to Chaos: Practical Bifurcation and Stability Analysis. Elsevier, New York.

Sokolinsky, V., Frostig, Y., 1997. Effects of boundary conditions in high-order buckling of sandwich panels with transversely flexible core. In: Proceedings of the Euromech 360 Colloquium on Mechanics of Sandwich Structures. Kluwer Academic Publishers, Saint-Etienne.

Sokolinsky, V., Frostig, Y., 1998. Nonlinear behavior of sandwich panels with a transversely flexible core — high-order theory approach. In: Sankar, B.V. (Ed.), Proceedings of the 1998 ASME International Mechanical Engineering Congress and Exposition, Recent Advances in Mechanics of Aerospace Structures and Materials, AD-Vol. 56. ASME, New York, pp. 193–206.

Sokolinsky, V., Frostig, Y., 1999. Boundary Conditions Effects in Buckling of "Soft" Core Sandwich Panels. Journal of Engineering Mechanics, ASCE 125 (8), 865–874.

Thomsen, O.T., Frostig, Y., 1997. Localized bending effects in sandwich panels: Photoelastic investigation versus high-order sandwich theory results. Composite Structures 37 (1), 97–108.

Zenkert, D., 1995. An Introduction to Sandwich Construction. Chameleon Press, London, UK.